Numerical simulation of micro flows with moving obstacles

Guillaume Dechristé, Luc Mieussens

Numerical simulation of micro flows with moving obstacles

G. Dechristé and L. Mieussens

Univ. Bordeaux, IMB, UMR 5251, F-33400 Talence, France. CNRS, IMB, UMR 5251, F-33400 Talence, France.

E-mail: Guillaume.Dechriste@math.u-bordeaux1.fr, Luc.Mieussens@math.u-bordeaux1.fr

Abstract. We present a numerical method for computing unsteady rarefied gas micro flows, in domains with moving boundaries, in view of applications to complex computations of moving structures in micro or vacuum systems. The flow is described by the Bhatnagar-Gross-Krook (BGK) model of the Boltzman equation. A standard approach to simulate incompressible viscous flows with moving boundaries is the immersed boundary method. In this work, we propose an extension of this approach to a deterministic simulation of rarefied flows. The immersed boundary approach consists in keeping the same mesh all along the calculation: every cell of the mesh remains fixed for all time steps while the domain occupied by the gas changes. This strategy avoids to use moving meshes and remeshing approaches, and should be easily applied to problems with complex geometries. The method has been tested with both specular and diffuse boundary conditions and has been validated on several 1D problems (moving piston, actuator, etc.). Up to our knowledge, this is the first time that a deterministic simulation method for rarefied flows with moving obstacles based on the immersed boundary method is presented.

1. Introduction

The standard approach used for the computation of rarefied gas flows is the Direct Simulation Monte Carlo [1]. For low-speed flows, the results obtained with this method are often noisy, which is a major drawback for the simulation of Microelectromechanical systems (MEMS). However when the Navier-Stokes solution is known, low-variance approaches have been recently proposed [2, 3] and it has been proved to be very efficient. An other approach to get more accurate results are the deterministic methods [4]. In order to reduce the numerical cost required by the computation of binary collisions, the Boltzmann equation is often replaced by the simpler BGK model [5].

Generally, problems involving moving obstacles are treated with remeshing methods. However, this approach needs high computational time and high numerical cost, especially for kinetic equations. Recently, Russo and Filbet [6] proposed a semi-langrangian scheme for one dimensional problems to avoid the remeshing approach.

A well-known Eulerian approach to simulate incompressible viscous flows with moving boundaries is the immersed boundary method [7]. This approach consists in solving the equation on a Cartesian grid. Even the solid part of the domain is meshed, but the equation is not solved in the solid cells. These cells are instead filled with a boundary condition value. The main difficulty is then to properly choose this condition. The advantages of this strategy are the

low computational cost and its natural extension to higher dimensions. Here, we propose an extension of this method to a deterministic simulation of rarefied flows based on the BGK model.

The outline of this article is the following. In section 2, we briefly present the kinetic description of a rarefied gas. Then, the application of the immersed boundary method is described in section 3. Finally, in section 4 the method is validated on two different test cases: a moving piston and an actuator.

2. Kinetic description of rarefied gas dynamics

Gas flows can be modelled either at a macroscopic or microscopic scale. Euler and Navier-Stokes equations describe the macroscopic behaviour of the flow, while the Boltzmann equation describes the flow at a microscopic scale. The level of rarefaction of a gas can be estimated through the Knudsen number (Kn), which is defined by the ratio between the mean free path (l) of the molecules and a characteristic macroscopic length of the system (L):

$$Kn = \frac{l}{L}. \tag{1}$$

Large Knudsen numbers correspond to a rarefied flow, while small Knudsen numbers indicate that the flow is close to the equilibrium and can be described by Euler or Navier-Stokes equations. It is generally admitted [1] that the macroscopic equations are no longer sufficient when the Knudsen number is greater than 0.1.

2.1. Boltzmann equation and BGK model

In kinetic theory, the basic model used for the description of the gas is the Boltzmann equation:

$$\partial_t f + \mathbf{v} \cdot \nabla_{\mathbf{x}} \cdot f = Q(f), \tag{2}$$

where f is the distribution function defined such that $f(t, \mathbf{x}, \mathbf{v})\mathbf{dxdv}$ is the mass of molecules located in the space volume $\mathbf{dx}$ with a velocity contained in an elementary volume $\mathbf{dv}$ at time t. The macroscopic quantities are therefore defined by the first moments of f:

$$\begin{pmatrix} \rho(t,\mathbf{x}) \\ \rho\mathbf{u}(t,\mathbf{x}) \\ E(t,\mathbf{x}) \end{pmatrix} = \int_{\mathbb{R}^d} \begin{pmatrix} 1 \\ \mathbf{v} \\ \frac{1}{2}|\mathbf{v}|^2 \end{pmatrix} f(t,\mathbf{x},\mathbf{v})\mathbf{dv}. \tag{3}$$

The temperature of the gas may be deduced from the conservative quantities though the relation $E = \frac{1}{2}\rho|\mathbf{u}|^2 + \frac{d}{2}\rho RT$ where d is the dimension of the velocity space and R is the gas constant, which is defined by the ratio between the Boltzmann constant and the molecular mass of the gas.

It is well known that in a thermodynamical equilibrium state, the distribution function f is equal to a Maxwellian distribution $\mathcal{M}(\rho, \mathbf{u}, T)$:

$$\mathcal{M}(\rho, \mathbf{u}, T) = \frac{\rho}{(2\pi RT)^{\frac{d}{2}}} \exp\left(-\frac{|\mathbf{v}-\mathbf{u}|^2}{2RT}\right). \tag{4}$$

The collision integral $Q(f)$ given by the Boltzmann operator [8] requires a very expensive computational cost. In order to avoid this problem, it is interesting to consider the simpler BGK model, proposed by Bhatnagar, Gross and Krook [5] where the collision term is modelled by a relaxation of the distribution function towards its corresponding Maxwellian equilibrium:

$$Q(f) = \frac{1}{\tau}\left(\mathcal{M}(\rho, \mathbf{u}, T) - f\right), \tag{5}$$

where τ is the relaxation time, defined by $\tau = \frac{\mu}{\rho RT}$. According to [1], $\mu = \mu_{ref}\left(\frac{T}{T_{ref}}\right)^{\omega}$ where μ_{ref}, ω and T_{ref} are constants that depend on the gas.

2.2. Boundary conditions

Boundary conditions may be modelled by two standard approaches: either specular or diffuse reflection. In the former model, incident molecules of velocity $\mathbf{v}$ are remitted with a velocity symmetric to $\mathbf{v}$ with respect to the wall. Consequently, if the wall moves at a velocity $\mathbf{u}_w$, the specular reflection condition will be given by the following relation:

$$f(t,\mathbf{x},\mathbf{v}) = f(t,\mathbf{x},\mathbf{v}-2(\mathbf{v}-\mathbf{u}_w)\cdot\mathbf{n}_\mathbf{x}\mathbf{n}_\mathbf{x}) \quad \text{if} \quad (\mathbf{v}-\mathbf{u}_w)\cdot\mathbf{n}_\mathbf{x} > 0, \tag{6}$$

where $\mathbf{n}_\mathbf{x}$ is the unit normal vector to the boundary, pointed to the gas.

In the diffuse reflection model, the molecules colliding with the boundary are remitted with a temperature T_w equal to the wall temperature and with a random velocity normally distributed around $\mathbf{u}_w$. This reads:

$$f(t,\mathbf{x},\mathbf{v}) = \phi\mathcal{M}(1,\mathbf{u}_w,T_w) \quad \text{if} \quad (\mathbf{v}-\mathbf{u}_w)\cdot\mathbf{n}_\mathbf{x} > 0, \tag{7}$$

where ϕ is defined such that the normal mass flux across the wall is zero:

$$\phi = -\frac{\int_{(\mathbf{v}-\mathbf{u}_w)\cdot\mathbf{n}_\mathbf{x}<0} f(t,\mathbf{x},\mathbf{v})(\mathbf{v}-\mathbf{u}_w)\cdot\mathbf{n}_\mathbf{x}\,\mathbf{dv}}{\int_{(\mathbf{v}-\mathbf{u}_w)\cdot\mathbf{n}_\mathbf{x}>0}\mathcal{M}(1,\mathbf{u}_w,T_w)(\mathbf{v}-\mathbf{u}_w)\cdot\mathbf{n}_\mathbf{x}\,\mathbf{dv}}. \tag{8}$$

2.3. Fluid limits of kinetic equation

Multiplying the Boltzmann equation (2) by $(1,\mathbf{v},\frac{1}{2}|\mathbf{v}|^2)$ and integrating it with respect to the velocity variable give the conservation laws:

$$\begin{aligned} \partial_t\rho + \nabla\cdot(\rho\mathbf{u}) &= 0,\\ \partial_t(\rho\mathbf{u}) + \nabla\cdot(\rho\mathbf{u}^2+\bar{\bar{p}}) &= 0,\\ \partial_t E + \nabla\cdot(E\mathbf{u}+\bar{\bar{p}}\mathbf{u}+\mathbf{q}) &= 0. \end{aligned} \tag{9}$$

This system can be closed if the gas is in equilibrium and in that case the stress tensor and the heat flux vector are

$$\bar{\bar{p}} = pI, \qquad \mathbf{q} = 0. \tag{10}$$

Equations (9) and (10) give the Euler equations of gas dynamics. For a regime close to the equilibrium, the Chapman-Enskog expansion leads to the Navier-Stokes equations with

$$\bar{\bar{p}} = pI - \mu[\nabla\mathbf{u} + (\nabla\mathbf{u})^T] - \mu_B(\nabla\cdot\mathbf{u})I, \qquad \mathbf{q} = -\kappa\nabla T, \tag{11}$$

where μ, μ_B and κ are the viscosity, the bulk viscosity and the thermal conductivity.

In order to make relatively fast numerical tests, this study is restricted to a simpler BGK model with one dimensional space variable x and one dimensional velocity variable v. In this case, the corresponding Navier-Stokes equations are easily calculated. Indeed, computing the moments of f naturally gives $\mu = 0$ and $\mu_B = 0$. Moreover, the heat flux vector can be calculated by a Chapman-Enskog expansion [9], and we get:

$$q = \frac{3}{2}\tau\rho R^2 T\partial_x T. \tag{12}$$

3. Immersed boundary method

Because the numerical tests are restricted to one dimensional cases, the following method will be described for a one dimensional flow. The computational domain is defined by $\Omega = [a, b]$ such that $\Omega = \Omega_{gas}(t) \cup \Omega_{solid}(t)$ where $\Omega_{gas}(t)$ represents the intervals occupied by the gas and $\Omega_{solid}(t)$ are the intervals filled by the walls at time t. Naturally, although Ω remains fixed for every times, $\Omega_{gas}(t)$ as well as $\Omega_{solid}(t)$ may vary in time when the obstacles are moving. With these definitions, equation (2) gives:

$$\begin{aligned} \partial_t f + v\partial_x f &= \frac{1}{\tau}(\mathcal{M}(\rho, u, T) - f) \qquad x \in \Omega_{gaz}(t), \\ f(t, x \in \partial\Omega_{gas}(t), v) &= f_w(t, x, v) \qquad (v - u_w) \times n_x > 0, \end{aligned} \tag{13}$$

where f_w is defined by equation (6) or (7).

3.1. Numerical method

The domain is discretized by a Cartesian grid of $(N + 1)$ nodes $x_{i+1/2} = i\triangle x$ with step $\triangle x = (b - a)/N$. The cells of the grid are denoted by $C_i = [x_{i-1/2}, x_{i+1/2}[$ and their center are $x_i = (i + \frac{1}{2})\triangle x$. At each discrete time step $t_n = n\triangle t$, we denote by $f_i^n(v)$ an approximation of the average of $f(t_n, x, v)$ over the cell C_i. Similarly, Ω_{gas}^n (resp. Ω_{solid}^n) denotes an approximation of $\Omega_{gas}(t)$ (resp. $\Omega_{solid}(t)$) and is defined by the union of the cells C_i whose center x_i are in $\Omega_{gas}(t)$ (resp. $\Omega_{solid}(t)$). Finally, we define the normal vector to the interface between a gas cell C_i and its neighbouring solid cell by:

$$\nu_i = \begin{cases} 1 \text{ if } C_{i+1} \in \Omega_{gas}^n \text{ and } C_{i-1} \in \Omega_{solid}^n \\ -1 \text{ if } C_{i-1} \in \Omega_{gas}^n \text{ and } C_{i+1} \in \Omega_{solid}^n \end{cases} . \tag{14}$$

For every cell in Ω_{gas}^n, we use the following standard first order upwind scheme:

$$f_i^{n+1} = f_i^n - \frac{\triangle t}{\triangle x}(\mathcal{F}_{i+\frac{1}{2}}^n - \mathcal{F}_{i-\frac{1}{2}}^n) + \frac{\triangle t}{\tau_i^n}(\mathcal{M}_i^n - f_i^n), \tag{15}$$

where the numerical flux at interface $x_{i+1/2}$ is defined by $\mathcal{F}_{i+1/2}^n = v^+ f_i^n + v^- f_{i+1}^n$, where $v^+ = \max(v, 0)$ is the positive part of v and $v^- = \min(v, 0)$ is the negative part of v. The calculation of this numerical flux at an interface between a gas cell C_i and a solid cell $C_{i-\nu_i}$ requires the value of $f_{i-\nu_i}^n$ for all $v \times \nu_i > 0$. For such velocities, there are two cases. First, if $(v - u_w) \times \nu_i > 0$, then we define $f_{i-\nu_i}^n$ by using the boundary condition (like in the ghost cell technique) and hence set $f_{i-\nu_i}^n$ to $f_{w,i-\nu_i}^n$ defined by:

- Specular reflection:
$$f_{w,i-\nu_i}^n(v) = f_i^n(v - 2(u_w - v)). \tag{16}$$
- Diffuse reflection:
$$\begin{aligned} &f_{w,i-\nu_i}^n(v) = \phi\mathcal{M}(1, u_w, T_w), \\ &\text{with} \quad \phi = -\frac{\int_{(v-u_w)\nu_i<0} \left(f_i^n(v)(v - u_x)\nu_i\right) dv}{\int_{(v-u_w)\nu_i>0} \left(\mathcal{M}(1, u_w, T_w)(v - u_w)\nu_i\right) dv}. \end{aligned} \tag{17}$$

At the contrary, if $(v - u_w) \times \nu_i < 0$, we propose to use the extrapolated value computed with the neighbouring gas cell C_i, that is to say we set $f_{i-\nu_i}^n(v) = f_i^n(v)$.

The velocity variable is approximated by using a discrete velocity method [10]. We define $f_{i,k}^n$ as an approximation of $f(t_n, x_i, v_k)$ where v_k are the nodes of a bounded Cartesian grid with

step $\triangle v$. The Maxwellian is approximated on this grid by a discrete Maxwellian which has the same moments as f. Then, equation (15) can be readily applied to the discrete velocity model where the flux ϕ for the diffuse boundary condition in equation (17) becomes:

$$\phi = -\frac{\sum\limits_{(v_k-u_w)\nu_i<0} f^n_{i-n_i,k}(v_k-u_w)\nu_i\triangle v}{\sum\limits_{(v_k-u_w)\nu_i>0} \mathcal{M}(1,u_w,T_w)(v_k-u_w)\nu_i\triangle v}. \tag{18}$$

If $v_k - 2(u_w - v_k)$ is not contained in the velocity grid, the value of $f_i(v_k - 2(u_w - v_k))$ for the specular reflection condition in equation (16) is calculated by a linear interpolation from $f_{i,K}$ and $f_{i,K+1}$ where K is defined by: $v_K < v_k - 2(u_w - v_k) \leq v_{K+1}$.

Positivity and conservative property of the scheme hold in a non-bounded domain under the CFL condition:

$$\Delta t < \min(\frac{\Delta x}{v_k}, \tau) \tag{19}$$

It would be desirable to get the stability of the scheme in a bounded domain. This property is directly linked to the mass conservation. We have not been able to get the total mass conserved in a simple fashion for now and we are currently working to solved the issue.

3.2. Transition solid cell/gas cell

In order to take into account the time variation of $\Omega_{gas}(t)$ and $\Omega_{solid}(t)$, a backward Euler scheme is applied for computing the movement of the boundary. This reads:

$$x_w^{n+1} = x_w^n + \triangle t \times u_w^n, \tag{20}$$

where x_w^n is an approximation of the boundary of $\Omega_{solid}(t^n)$. After the computation of f_i^{n+1} in $C_i \in \Omega^n_{gas}$ by equation (15), x_w^{n+1}, Ω^{n+1}_{gas} and Ω^{n+1}_{solid} are calculated. For simplicity, assume that $\nu_i = 1$. It may happen that a gas cell C_i becomes a solid cell if $x_w^{n+1} > x_i > x_w^n$. Even if f_i^{n+1} is calculated there, its value becomes useless for the next time step. Similarly, a solid cell C_i may become a gas cell if $x_w^{n+1} < x_i < x_w^n$. In that case, the value of f_i^{n+1} is required for computing the next time step. We propose to use the extrapolated value computed with the neighbouring gas cell C_{i+1}, that is to say we set $f_i^{n+1} = f_{i+1}^{n+1}$.

The method can be summarized in four steps:

- Calculation of the numerical flux at all interfaces between gas cells and solid cells.
- Calculation of f_i^{n+1} in all cells $C_i \in \Omega^n_{gas}$.
- Computation of Ω^{n+1}_{gas} by the calculation of x_w^{n+1}.
- Computation of f_i^{n+1} in the new gas cells.

We emphasize that the presented method is reduced to the standard scheme described in [10] for non-moving boundaries. Moreover, the principal advantage of the method is that the only difference between moving and non-moving boundaries is the implementation of the boundary following. This implementation can be easily extended to higher dimension thank to level set methods. The main drawback of this method is that we don't know yet how to implement the conservation of the total mass conservation for internal flows.

4. Numerical comparisons

The method described above has been validated with two test cases: a moving piston and an actuator. A convergence study has been led for each case, and it has been shown that the immersed boundary method fully preserves the first order accuracy of scheme (15) used to discretize the transport equation.

4.1. Moving piston

We consider a domain of total length $L = 20$ with a piston moving at velocity $\sin(t)$ at the left edge of the domain. The variables are initialized as follows:

$$u = 0, \qquad \rho = 1, \qquad RT = 1, \qquad x_{piston}(t = 0) = 2. \tag{21}$$

For all the following simulations, the domain has been discretized by 2000 cells ($\Delta x = 2 \cdot 10^{-2}$). The time step is chosen according to (19) and its the order of magnitude is 10^{-5}. The computation lasts less than 5 minutes for each case on an Intel Xeon CPU X5560, 2.80GHz.

First, the velocity of the gas near the piston is the same as the velocity of the piston. The specular boundary condition (16) is implemented with $u_w = \sin(t)$. The solution of the BGK equation (2) with specular boundary conditions (6), is compared to the solution of Euler equations (9) and (10). In order to ensure the compatibility of the two models, the simulations are performed in the context of small Knudsen number ($\tau = 10^{-3}$). Euler equations are written in Lagrangian coordinates [11] and solved by using the central scheme of Nessayhu-Tadmor [12]. A shock wave is created by the motion of the piston and propagates inside the gas. A rapid changed of the density and temperature can be observed when the piston is changing its way. The profiles of density and temperature are plotted on figure 1 after the piston has moved forward and backward.

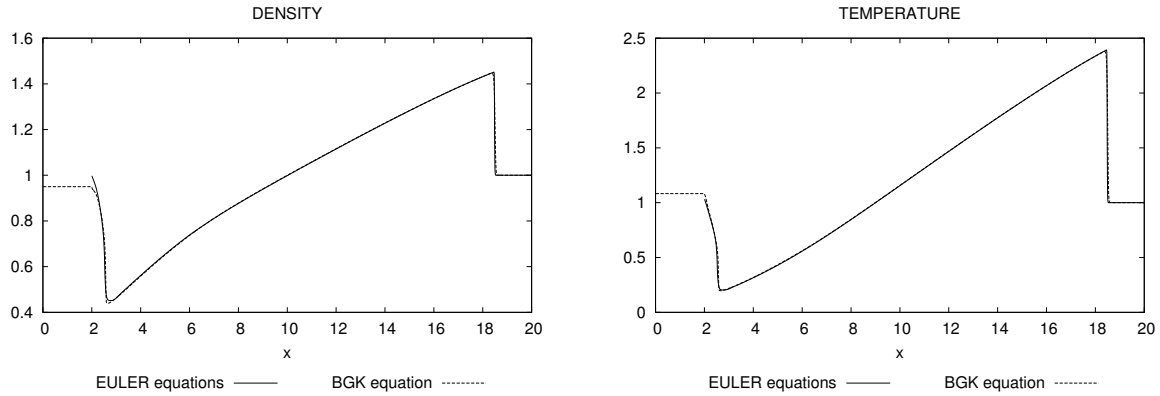

Figure 1. Comparison between Euler and BGK equations. Density and temperature profiles at $t = 2\pi$.

Second, the temperature of the gas close to the piston is set to the temperature of the piston by using diffuse boundary condition (17), with $u_w = \sin(t)$ and $T_w = 1$. Results obtained with the BGK equation (2) associated now with diffuse reflection boundary conditions (7), are compared with results obtained with Navier-Stokes equations, eq. (9) and (11). Here, again, the Navier-Stokes equations are written in Lagrangian coordinates and solved with the central scheme. The results are quite similar to the previous case, except that the density near to the piston increases a lot. Density and temperature are plotted on figure 2 after the first compression.

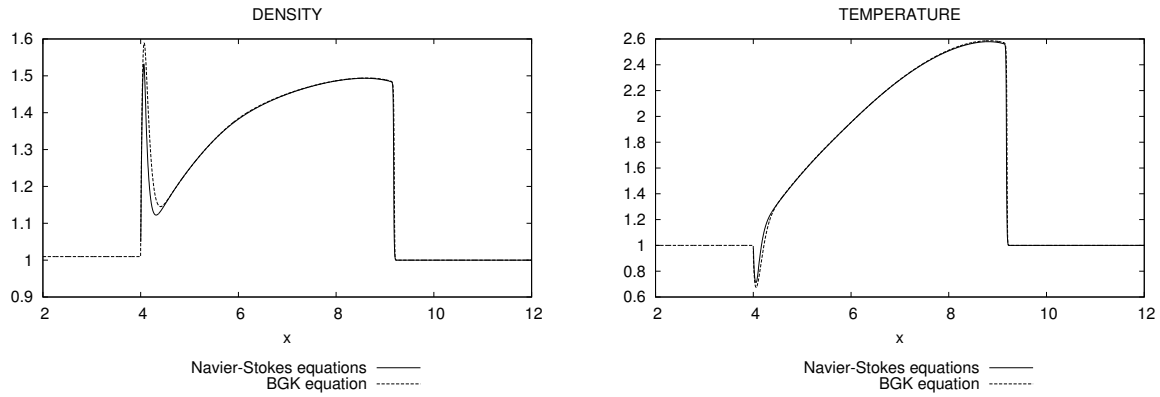

Figure 2. Comparison between Navier-Stokes and BGK equations. Zoom of density and temperature profiles at $t = \pi$.

Note that the computational domain of the BGK computation differs from the computational domain of Euler equations. Indeed, the former equation has been computed on a fixed domain (immersed boundary method) while the computation of the latest set of equations is done on a domain moving with the gas (equations written in Lagrangian coordinates). The same remark can be done for the comparison between BGK and Navier-Stokes equations.

The good agreement between the solution of the BGK equation and the predictions of Euler and Navier-Stokes equations ensure that the immersed boundary method is accurate when the velocity of the moving object is independent of the behaviour of the gas. Indeed, in this test case the piston moves whatever the state of the gas is.

In the following, we study a case where the interaction between the gas and the wall is more complex.

4.2. Actuator

A flat plate is contained in a slab. At initial time, the temperature, the pressure and the density are the same in the whole domain and are denoted by T_0, P_0 and ρ_0. The right side of the plate is heated to T_w whereas the left side is maintained at the initial temperature T_0 of the gas. In the same way, the right wall of the slab is heated and the left wall is kept to the initial temperature. The experiment is illustrated in figure 3. Because the gas is heated close to the right side of the plate, the temperature and the pressure increase there and the movement of the plate is induced by the pressure difference between the two sides.

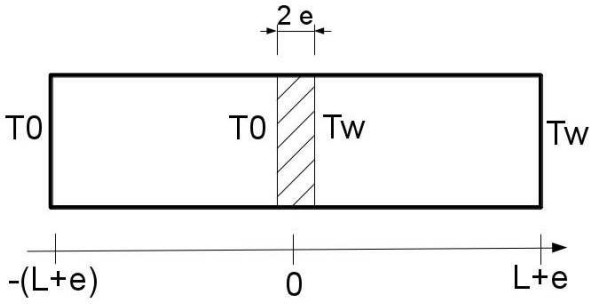

Figure 3. Schematic view of the actuator.

The equilibrium state of the gas and the equilibrium position of the plate can be easily calculated. Once the equilibrium state is reached, temperature, pressure and density are constant in each part of the slab. The state of the gas can be fully described with the perfect gas relation and the mass conservation. Indeed, denoting by P_{equi} and ρ_{left} (resp. ρ_{right}) the equilibrium pressure and left (resp. right) density and by x_{equi} the coordinate of the center of the plate once equilibrium is reached, we get:

- on the left side:

$$\left\{ \begin{array}{l} \rho_0 R T_0 = P_0 \\ \rho_{left} R T_0 = P_{equi} \\ \rho_0 L = \rho_{left}(L + x_{equi}) \end{array} \right. \Longrightarrow P_{equi} = \frac{L}{L + x_{equi}} P_0. \tag{22}$$

- on the right side:

$$\left\{ \begin{array}{l} \rho_0 R T_0 = P_0 \\ \rho_{right} R T_w = P_{equi} \\ \rho_0 L = \rho_{right}(L - x_{equi}) \end{array} \right. \Longrightarrow P_{equi} = \frac{T_w}{T_0} \frac{L}{L - x_{equi}} P_0. \tag{23}$$

From equations (22) and (23), it comes:

$$x_{equi} = L \frac{1 - T_w/T_0}{1 + T_w/T_0}, \qquad \rho_{left} = \frac{P_{equi}}{R T_0}, \qquad \rho_{right} = \frac{P_{equi}}{R T_w}. \tag{24}$$

The immersed boundary method is used for the simulation of this experiment. The domain is discretized by 800 cells ($\Delta x = 2.5 \cdot 10^{-2}$). The BGK equation (2) is solved with diffuse boundary conditions (7). The velocity of the plate is calculated through the fundamental principle of dynamics with an external force corresponding to the difference of pressure at each side of plate:

$$m \frac{du_w}{dt} = (P_{left} - P_{right}) S, \tag{25}$$

where m and S are the mass and the area of plate.

At initial time, the domain is filled with argon. $P_{left} = P_{right} = P_0$ and the velocity of the plate is $u_w = 0$. With these parameters, the Kundsen number, based on a characteristic length scale set to 2, is equal to $8 \cdot 10^{-2}$. Since the temperature at the right side of the slab increases, the pressure increases too, and the piston moves from the right side to the left side with a positive acceleration. There is a time at which $P_{left} = P_{right}$, and hence $\frac{du_w}{dt} = 0$. But since $u_w \neq 0$, the plate keeps on moving. As a result, it will evolve toward the equilibrium point by oscillating around it. These oscillations are observed on figure 4 in which the velocity of the center of the plate is plotted. The results are obtained after 24 hours of computation on an Intel Xeon CPU X5560, 2.80GHz. Computations have been launched for several Knudsen numbers (0.04, 0.8 and 10) and the oscillatory behaviour of the plate has been observed in each case.

Taking $T_0 = 270$ K, $T_w = 330$ K and $P_0 = 10$ Pa, the error of the simulated equilibrium position with respect to the exact equilibrium position is equal to 5% . Indeed, the value of the exact equilibrium position comes from equations (24): $x_{equi}^{exact} = -0.1$. The predicted equilibrium position is calculated by the average between the center of the leftmost and the rightmost solid cells at time $t = 7$: $x_{equi}^{predicted} = -0.105$ (Fig. 5).

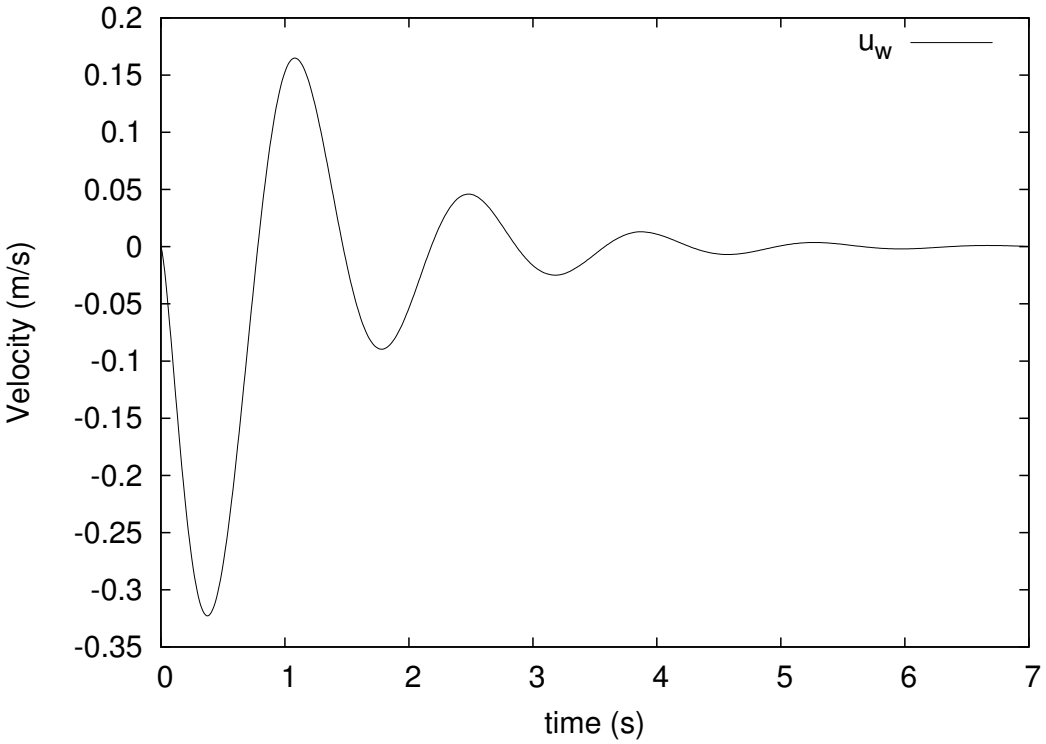

Figure 4. Velocity of the moving plate.

Moreover, the error of the predicted pressure ($P_{equi}^{predicted} = 11.15Pa$) with respect to the exact pressure ($P_{equi}^{exact} = 11.11$) is 3.6%. The errors for the right and left density are in the same order of magnitude (3% and 3.1%).

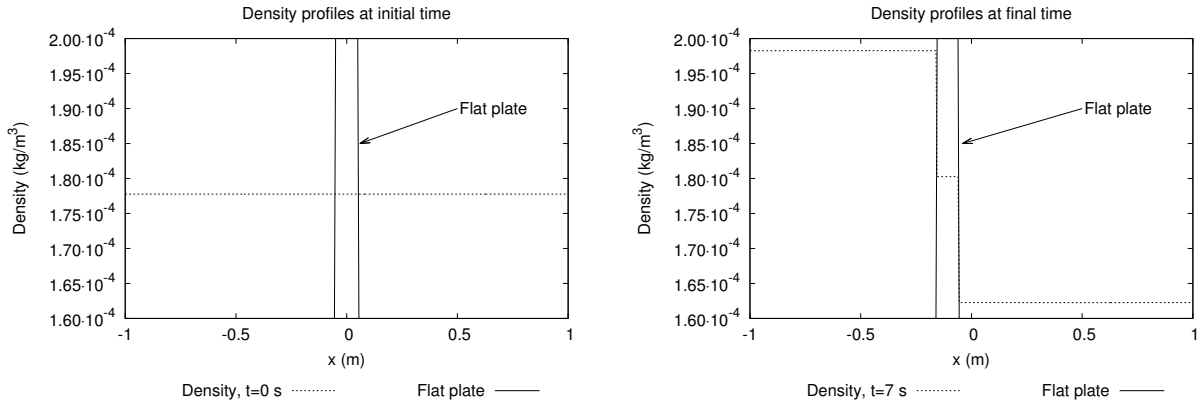

Figure 5. Density profiles and position of the flat plate at initial time ($x = 0$) and equilibrium time ($x = -0.101$).

5. Conclusion

We proposed an extension of the immersed boundary method, already used for the simulation of incompressible viscous flows, to the simulation of the BGK model of gas dynamics. The method has been validated for one dimensional problems and we showed that the method accurately

predicts the behaviour of the gas near the boundary. The interaction between gas and solid boundaries is well predicted. The application of our method to higher dimensional problems will be presented in a forth coming work. In particular, our project is to use this approach to study the radiometric effect.

References

[1] Bird G A 1994 *Molecular Gas Dynamics and the Direct Simulation of Gas Flows* (*Oxford Engineering Science Series* vol 42) (Oxford Science Publications)
[2] Baker L and Hadjiconstantinou N 2005 *Physics of Fluids* **17** 1–4
[3] Homolle T and Hadjiconstantinou N 2007 *Journal of Computational Physics* **226** 2341–2358
[4] Buet C 1996 *Transport Theory and Statistical Physics* **25** 33–60
[5] Bhatnagar P L, Grosss E P and Krook M 1954 *Physical Reeview* **94** 511–525
[6] Russo G and Filbet F 2009 *Kinetic and related models* **2** 231–250
[7] Dong H, Mittal R and Najjar F 2006 *Journal of Fluid Mechanics* **566** 309–343
[8] Sone Y 2007 *Molecular Gas Dynamics. Theory, Techniques and Applications.* Modeling and Simulation in Science, Engineering and Technology (Birkhause)
[9] Chapman S and Cowling T G 1970 *The mathematical theory of non-uniform gases* (Cambridge University press)
[10] Mieussens L 2000 *Mathematical Models and Methods in Applied Sciences* **10** 1121–1149
[11] Godlewski E and Raviart P A 1996 *Numerical Approximation of Hyperbolic System of Conservation Laws* (*Applied Mathematical Sciences* vol 118) (Springer)
[12] Nessyahu H and Tadmor E 1990 *Journal of Computational Physics* **87** 408–463